Journal of Alloys and Compounds 785 (2019) 7–12

Contents lists available at ScienceDirect

Journal of Alloys and Compounds

journal homepage: http://www.elsevier.com/locate/jalcom

N-doped reduced graphene oxide supported Cu_2O nanocubes as high active catalyst for CO_2 electroreduction to C_2H_4

Hui Ning [a], Qinhu Mao [a], Wenhang Wang [a], Zhongxue Yang [a], Xiaoshan Wang [a], Qingshan Zhao [a], Yan Song [b], Mingbo Wu [a, *]

[a] State Key Laboratory of Heavy Oil Processing, Institute of New Energy, College of Chemical Engineering, China University of Petroleum (East China), Qingdao 266580, China
[b] CAS Key Laboratory of Carbon Materials, Institute of Coal Chemistry, Chinese Academy of Sciences, Taiyuan 030001, China

ARTICLE INFO

Article history:
Received 5 November 2018
Received in revised form
5 January 2019
Accepted 12 January 2019
Available online 14 January 2019

Keywords:
N-doped graphene
Cuprous oxide
Electroreduction
Carbon dioxide
Ethylene

ABSTRACT

Electrocatalytic carbon dioxide reduction (CO_2RR) to high value-added chemicals is a promising technology to address greenhouse effect and energy challenges. As ethylene is a desirable product of CO_2RR with great economic value, herein, we proposed a facile method to in situ loading cuprous oxide (Cu_2O) nanocubes on nitrogen doped reduced graphene oxide (NRGO) to fabricate a Cu_2O/NRGO composite under ambient conditions, which exits a high faradaic efficiency of ethylene (19.7%) at −1.4 V (*vs.* reversible hydrogen electrode) with stable current density of 12 mA cm^{-2}. The mass activity of Cu_2O supported on NRGO towards C_2H_4 formation reaches as high as 136.1 mmol h^{-1} g^{-1}, which is more than 24-folds of pristine Cu_2O. SEM images reveal that Cu_2O with perfect cubic morphology are highly dispersed on NRGO, promoting the exposure of active sites for CO_2RR. Additionally, the pyridinic-N in NRGO was supposed to behave synergistic effect with Cu_2O, leading to a clearly improvement of activity and durability of Cu_2O for electrocatalytic CO_2 reduction to ethylene. Our work provides a useful strategy to enhance the catalytic performance of copper catalysts for CO_2RR by using nitrogen doped carbon materials as supports.

1. Introduction

Electrocatalytic carbon dioxide reduction reaction (CO_2RR) to valued chemicals offers a promising route towards mitigating the greenhouse effect and carbon dioxide utilization [1–4]. In a typical 0.1 M $KHCO_3$ aqueous solution, CO_2 can be electro reduced to various C_1, C_2 and C_3 products, of which C_2H_4 is a desirable product with significant economic value. However, the development of CO_2RR to C_2H_4 is hampered by the lack of efficient catalysts.

Up to now, screened materials have been investigated as catalysts for CO_2 electroreduction but only copper-based catalysts behave comparatively higher selectivity towards C_2H_4 [5–7]. As a vastly used semiconductor material, Cu_2O has drawn much attention in solar cells and diode [8–12]. Zang et al. explored Cu_2O nanowires with triangular and hexagonal cross sections of a series of diameter size, and found obvious spatially separated charge distribution of conduction and valance band edges, ensuring long lifetime of excited electron-hole pairs that may greatly benefit performance of optoelectronic devices [13]. Recently, cuprous oxide (Cu_2O) has drawn much attention because of its higher selectivity to C_2H_4. The Cu−O vacancy in the partial reduction Cu_2O crystals are considered to be the main active sites for ethylene formation during CO_2RR. However, the activity and stability of Cu_2O is still not satisfactory. One major problem is the easy aggregation of pristine Cu_2O nanoparticles, which significantly hampers the exposure of active sites on the surface of Cu_2O crystals. Another one is the corruption of Cu_2O nanocrystals in long-term CO_2RR process due to the reduction of Cu(I) to Cu(0) [14,15]. It has been proved that building composites is an effective strategy to enhance the catalytic performance of metal oxide materials for electrochemical applications [16,17]. Due to the special sp^2C structure, high conductivity and large surface area, graphene materials have been widely used as supports to fabricate composites with metal oxides as high efficient electrocatalysts [18]. Doping with nitrogen atoms, the obtained nitrogen doped graphene (NG) not only has intrinsic activity for electrochemical reduction of CO_2, but also helps to improve the catalytic performance of metal oxides as supports [19,20]. Sun et al. [21] reported a Cu/C composite, in which

* Corresponding author.
E-mail address: wumb@upc.edu.cn (M. Wu).

https://doi.org/10.1016/j.jallcom.2019.01.142
0925-8388/

monodispersed Cu nanoparticles (NPs) were assembled on a pyridinic-N rich graphene (p-NG). Used as catalyst for CO_2RR, the pyridinic-N acted as CO_2 and proton absorbers, facilitating hydrogenation of CO_2 with further carbon–carbon coupling reactions on Cu to generate C_2H_4. By density functional theory calculation, Chen et al. [22] proved copper atom had stronger interactions with p-NG compared to graphene due to the change of electronic structures around the doped nitrogen atom, which may help to explain why abundant nitrogen moieties in p-NG can help to fix the position of Cu NPs and inhabit its aggregation. Agnoli et al. [23] prepared a NG-Co_3O_4 composite as catalyst for CO_2RR to formic acid. It was found the pyridinic-N functionalities in NG may coordinate Co centers to stabilize the morphology of CoO, the true active phase reduced from Co_3O_4 during CO_2RR. Rondinone et al. [24] synthesized a highly textured N-doped carbon nanospike film (CNS), which had a similar structure to multilayer graphene. As support for Cu NPs, the Cu/CNS hybrids presented a relatively high faradaic efficiency of 63% towards ethanol for CO_2RR. With the help of electrochemical analysis and density functional theory (DFT) calculation, synergistic effects were proved between pyridinic-N and Cu in bonding with OCCO, an important C_2 intermediate, in which the two oxygen atoms may covalently bound on the reactive Cu and less reactive CNS separately to provide a pathway towards selective formation of ethanol during CO_2 reduction. The above reported synergistic effects between Cu and NG enlighten us on selecting NG as support to improve the activity and stability of Cu_2O for electrocatalytic CO_2RR to ethylene.

Herein, we put forward a facile method to prepare Cu_2O/nitrogen doped reduced graphene oxide composites as catalysts for CO_2 electroreduction. Results showed that the activity and stability of Cu_2O towards ethylene formation was greatly improved and the corresponding mechanism was also investigated.

2. Experiment

2.1. Materials and reagents

Graphene oxide (GO) was obtained from Nanjing XFNANO Materials Tech Co., Ltd., P.R. China. Copper chloride dehydrate (purity, 99.0%), melamine (purity, 99.99%), potassium hydrogen carbonate (purity, 99.5%), ethanol anhydrous (purity, 99.7%), sodium hydroxide (purity, 96.0%), and L-ascorbic acid (purity, 99.99%) were purchased from Sinopharm Chemical Reagent Co., Ltd., P. R. China. All the reagents were used as received without further purification. The deionized water (>15 MΩ) in all experiments was made by a Millipore system in our lab.

2.2. Preparation of RGO and NRGO

Typically, GO and melamine (1:5, mass ratio) were simultaneously added into deionized water followed by sonication for 2 h. Then the solution was dried under 60 °C until water was evaporated to obtain a solid mixture, which was subsequently heated at 900 °C under nitrogen atmosphere for 3 h with a ramp rate of 15 °C min^{-1} in a temperature-programmed tube furnace. After cooling down to room temperature, the resultant black powder was washed with deionized water thoroughly to remove any impurities and recollected by vacuum filtration. After freeze-drying for 48 h, the nitrogen doped reduced graphene oxide was obtained, denoted as NRGO. The RGO were synthesized with the same procedure without adding melamine.

2.3. Preparation of Cu_2O/NRGO, Cu_2O/RGO and Cu_2O

As illustrated in Fig. 1, the synthesis of Cu_2O/NRGO was described as follows: Firstly, 1.2 mL of 0.05 M $CuCl_2 \cdot 2H_2O$ aqueous solution was dropwise added into 4.0 mL of NRGO aqueous solution (concentration, 1.0 mg/mL) and stirred for 2 h to obtain solution A. Then, 1.8 mL of 0.2 M NaOH solution was slowly added into solution A to get a suspension, denoted as solution B. With further adding 5.0 mL of 0.02 M ascorbic acid into solution B and stirred for 2 h at room temperature, the precipitate was collected by vacuum filtration and washed with deionized water and ethanol thoroughly to obtain a black powder, which was subsequently dried at 60 °C for 4 h under vacuum to get Cu_2O/NRGO. Following the same procedure, Cu_2O/RGO was synthesized by replacing NRGO with RGO. As a control experiment, Cu_2O was prepared with the same procedure without adding any carbon materials in solution A.

2.4. Characterization

The scanning electron microscopy (SEM) images of all samples as made were measured on Hitachi S-4800 (Japan). The X-ray diffraction (XRD) patterns were recorded on an X'Pert PRO MPD diffractometer (Netherlands) at 40 kV and 40 mA with Cu Kα radiation. The surface elemental compositions were collected by an X-ray photoelectron spectroscopy (XPS, Thermo Scientific Escalab 250XI, America) with Al Kα radiation. The Raman spectra were recorded on Renishaw RM2000 (512 nm laser, Britain).

2.5. Electrochemical reduction of CO_2 and products analysis

Electrochemical studies of catalysts as made for CO_2RR were conducted at an electrochemical workstation (CHI 760, Shanghai CH Instruments Co., P. R. China) in a H-type cell with two-compartments separated by a proton exchange membrane (Nafion 117, Dupont). The electrolyte in all experiments was 30 mL of 0.1 M $KHCO_3$ aqueous solution. A potassium chloride saturated Ag/AgCl and a platinum sheet (1 × 1 cm^2) were equipped as the reference and the counter electrodes, respectively.

The working electrode was prepared as follows: 1.0 mg as-prepared catalyst was mixed with 200 μL ethanol under

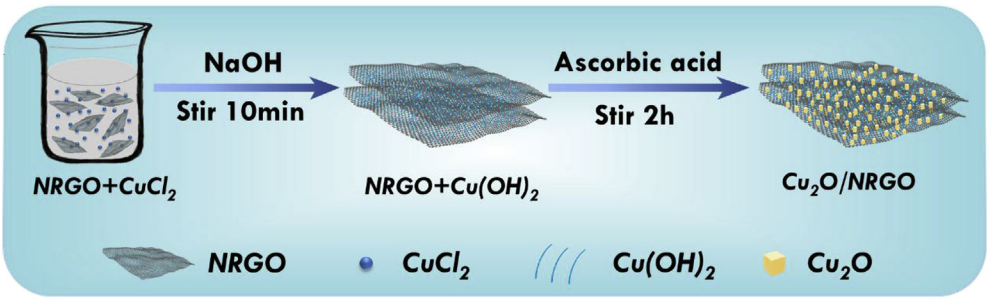

Fig. 1. Illustration for the synthesis of Cu_2O/NRGO.

ultrasonic for 10 min, following by adding 3.0 μL 5 wt% Nafion solution (DuPont) to obtain a suspension. After ultrasonic for another 30 min, a L-type glassy carbon electrode (ø = 10 mm) was smeared with the dispersed suspension and dried with N_2.

Before testing, the electrolyte in cathode side was bubbled with Ar for 30 min to exclude air, followed by saturated with high purity CO_2 (99.999%) for another 30 min. During electrochemical measurements, CO_2 gas flow was controlled at 20 mL/min. The gas-phase products generated during CO_2 electrolysis at each fixed potential were quantitatively analyzed by a gas chromatography (BFRL-3420A, China), which was online connected with head space of the cathodic side of electrochemical cell. The gas samples were injected to GC using a ten-port valve system with high purity Ar (99.999%) as carrier gas. The GC system was equipped with two columns associating with two detectors respectively. The thermal conductivity detector (TCD) was installed to detect hydrogen and carbon monoxide while the flame ionization detector (FID) was fabricated to detect hydrocarbons. Taking ethylene as our target product, the scope of this work was restricted to gas phase products. The faradaic efficiency (FE) of all gas products was calculated according to the methods reported by Yeo et al. [15]. All the work potentials in the text were referred to the reversible hydrogen electrode (RHE) using the following equation: $E_{(RHE)} = E_{(Ag/AgCl)} + 0.197\ V + (0.059 \times pH)$ [25]. The pH value of CO_2 saturated electrolyte is *ca.* 6.8.

3. Results and discussion

The XRD patterns of GO, RGO and NRGO were depicted in Fig. 2. The diffraction peak at $2\theta = 10.3°$ in Fig. 2a was identified as a characteristic peak of GO corresponding to an interlayer distance of 0.86 nm, which is consistent with previous reported [26–28]. After pyrolysis at high temperature, the peak at 10.3° disappeared completely while a new diffraction peak at $2\theta = 26.0°$ of RGO and NRGO appeared, demonstrating the successful reduction of GO. For Cu_2O/RGO and Cu_2O/NRGO, peaks at 29°, 36°, 42°, 52°, 61° and 73° are indexed to (110), (111), (200), (211), (220) and (311) planes of Cu_2O nanoparticles (JCPDS PDF#77-0199) respectively, indicating Cu_2O were successfully prepared and in-situ supported on the carbon materials.

SEM images showed both RGO (Fig. 3a) and NRGO (Fig. 3b) had ultra-thin two-dimensional structures. Fig. 3c and d confirmed that Cu_2O supported on RGO and NRGO presented well-defined cubic morphology, as well as pristine Cu_2O (Fig. S1). The average size of pristine Cu_2O is *ca.* 120 nm (Fig. S1). While the average size of Cu_2O on RGO and NRGO is *ca.* 64 nm and *ca.* 90 nm respectively, indicating RGO and NRGO inhibit the growth of Cu_2O nanocrystals.

The structural deformations of GO, RGO and NRGO were evaluated by Raman spectroscopy. As shown in Fig. S2, the characteristic D-band at 1335 cm^{-1} (associated with structural defects of sp^2C) and G-band at 1590 cm^{-1} (related to in-plane vibrational of sp^2C) were identified in GO, RGO and NRGO patterns. It is generally agreed that the intensity ratio of D-band to G-band (I_D/I_G) reveals the degree of structural defects in graphene material. The I_D/I_G of three graphene materials followed the order: NRGO (1.31) > RGO (1.18) > GO (0.89). Compared with GO, the increasing I_D/I_G of RGO is ascribed to the loss of carbon atoms due to the decomposition of oxygen-functional groups during pyrolysis procedure [29]. Besides that, due to incorporation of N heteroatoms, NRGO presents the highest value of I_D/I_G among all the three carbon materials [26].

The nitrogen species with other elements in GO, RGO, NRGO, Cu_2O/RGO and Cu_2O/NRGO were investigated by X-ray photoelectron spectroscopy (XPS). The chemical compositions of above five materials were listed in Table S1. It can be seen that the O content in RGO and NRGO is much less than GO, indicating GO was successfully reduced by heat treatment under inert atmosphere. As shown in Fig. 4a, four characteristic peaks corresponding to C 1s, O 1s, N 1s and Cu 2p were observed in Cu_2O/NRGO, confirming nitrogen was successfully incorporated into the carbon framework and Cu_2O was successfully anchored on NRGO. Despite some Cu(I) having been oxidized into Cu(II) during the tests, the XRD patterns indicated the copper materials as made still remain in pure Cu_2O phase [30]. For Cu_2O/RGO, no peaks of N1s but the characteristic peak of Cu 2p was clearly observed, indicating all the nitrogen atoms in NRGO were derived from melamine while not from GO.

Fig. 4b showed the details of binding energy of N species in Cu_2O/NRGO. Three main peaks resolved at 398.3, 400.0 and 401.2 eV were corresponded to pyridinic-N (1.82 at%), pyrrolic-N (0.57 at%) and quaternary-N (2.81 at%), respectively. The quaternary-N groups have been proved to enhance the electronic conductivity of graphene while the pyridinic-N at basal planes has relatively high binding energy with Cu^{2+} in the solution [22], promoting the in-situ growth of Cu_2O nanocubes on NRGO. It is worth noting that Cu_2O/RGO behave a little higher content of Cu than Cu_2O/NRGO, which may be ascribed to the aggregation of Cu_2O nanocubes (as depicted in Fig. 3c). As a result, it can be concluded that the nitrogen moieties doped in graphene play a key role in inhabiting the aggregation of Cu_2O nanocubes. This special phenomenon may be applied to synthesize other highly dispersed metal oxide nanoparticles as catalysts for specific reactions.

The catalytic performance of all the materials as made were recorded under different potentials from −1.0 V to −1.5 V *vs.* RHE. It can be seen from Fig. S4 that NRGO had a similar catalytic performance with RGO. The FE of CO on RGO and NRGO reached the maximum value of 7.1% and 6.9% respectively at −1.1 V *vs.* RHE, while hydrogen evolution reaction (HER) is the main competitive reaction to produce amount of H_2. No other gas products were

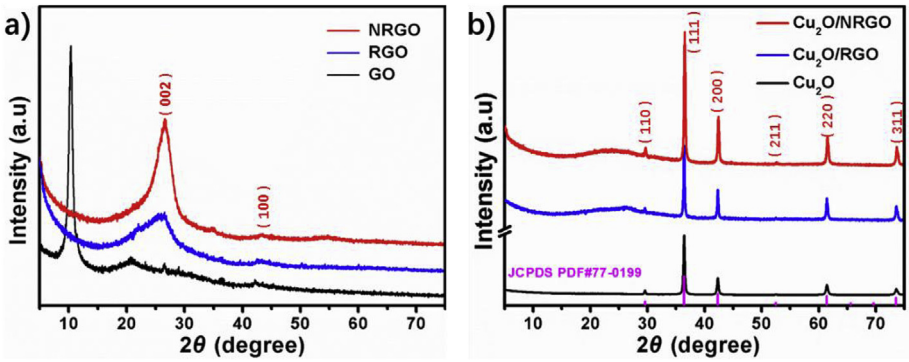

Fig. 2. XRD patterns of a) GO, RGO and NRGO, b) Cu_2O, Cu_2O/RGO and Cu_2O/NRGO.

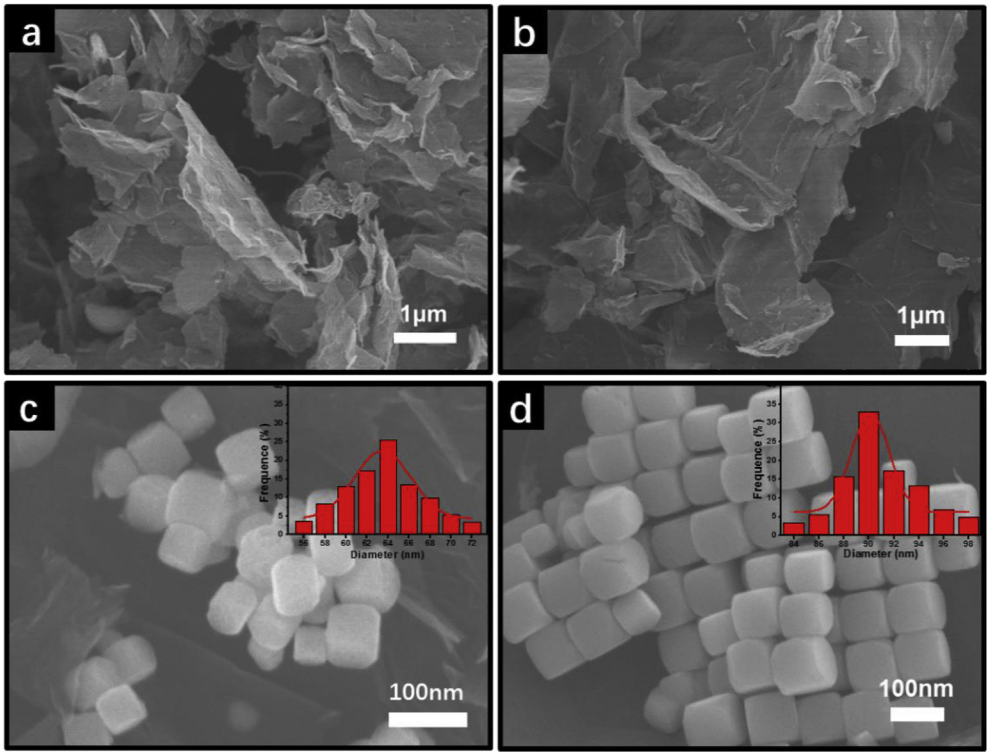

Fig. 3. SEM images of a) RGO, b) NRGO, c) Cu_2O/RGO and d) Cu_2O/NRGO.

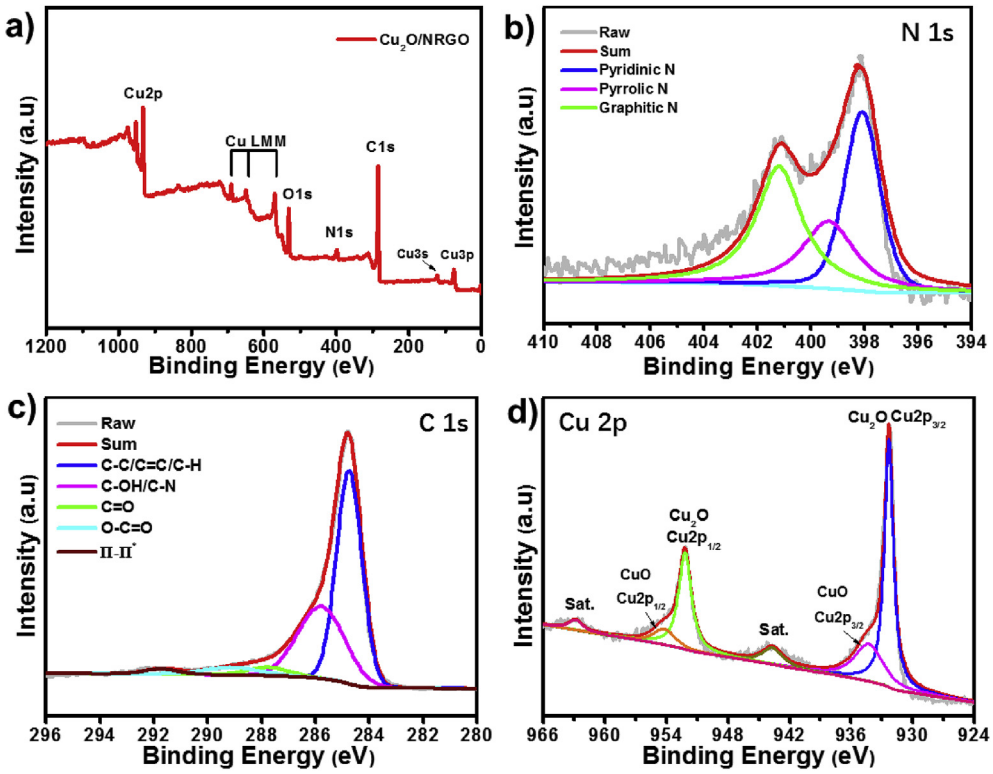

Fig. 4. XPS spectra of Cu_2O/NRGO. a) Full spectra, b) N 1s, c) C 1s and d) Cu 2p.

detected during the reactions, which means neither RGO nor NRGO can catalyze CO_2 electroreduction to ethylene. Therefore, the Cu_2O nanocubes in Cu_2O/RGO and Cu_2O/NRGO composites are the active sites for ethylene generation from CO_2RR.

The catalytic performances of Cu_2O/NRGO, Cu_2O/RGO and pristine Cu_2O were shown in Fig. 5. Along with the increasing potential, the FE of C_2H_4 on all the three catalysts increased gradually and reached the highest value at −1.4 V *vs.* RHE, whereas Cu_2O/NRGO had

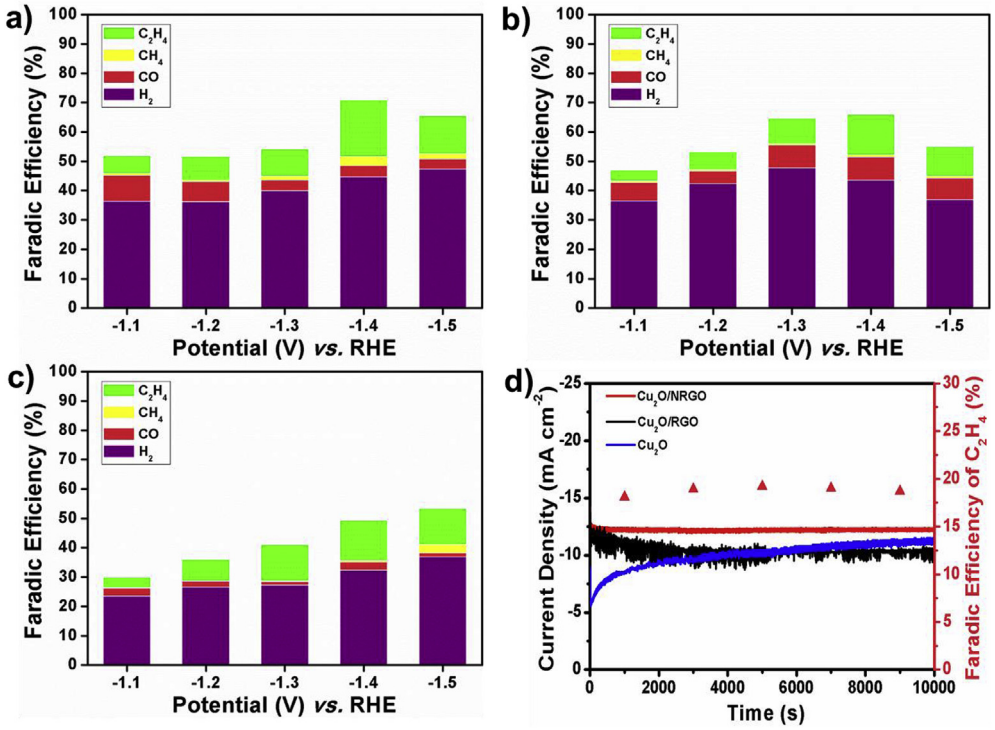

Fig. 5. The FE of all gas products on a) Cu_2O/NRGO, b) Cu_2O/RGO and c) Cu_2O. d) I-t curves of Cu_2O/NRGO, Cu_2O/RGO and Cu_2O with the FE of C_2H_4 on Cu_2O/NRGO (▲) at −1.4 V *vs.* RHE.

the highest value of 19.7%. The mass activity towards ethylene based on the mass of Cu_2O is also calculated at −1.4 V *vs.* RHE, as listed in Table S2. The mass activity of pure Cu_2O was 5.6 mmol h^{-1} g^{-1}. When supported on RGO, the mass activity of Cu_2O was raised to 84.3 mmol h^{-1} g^{-1}, which is ascribed to efficient exposure of active sites of Cu_2O. Interestingly, the mass activity of Cu_2O supported on NRGO reached as high as 136.1 mmol h^{-1} g^{-1}, indicating the nitrogen functionalities in NRGO further enhanced the activity of Cu_2O. Previous reports have proved the pyridinic-N functionalities in NRGO acted as a CO_2 and proton absorber during CO_2RR to facilitate hydrogenation and carbon–carbon coupling reactions on Cu active sites [21]. Yeo et al. [15] have previously demonstrated that Cu_2O was reduced rapidly and remained as metallic Cu^0 particles during the CO_2 reduction by in situ Raman spectroscopy and the oxide-derived copper (ODCu) is the real catalytic active species for reducing CO_2. Therefore, we suppose the high activity of Cu_2O on NRGO was ascribed to the plenty pyridinic-N moieties.

To further study the catalytic stability of Cu_2O/NRGO, Cu_2O/RGO and Cu_2O catalysts, long-term electrolysis of CO_2 tests was carried out at −1.4 V *vs.* RHE for 10,000 s. As depicted in Fig. 5d, due to the reduction of Cu_2O under negative potentials [15], the current density of pristine Cu_2O catalysts increased as time flows. Due to the strong anchoring nature of defects to Cu [31], the stability of Cu_2O on RGO was improved. It is worth noting that Cu_2O on NRGO displayed the best durability among the three catalyst as made. We suppose the pyridinic-N of NRGO can further improve the stability of Cu_2O due to the special pyridinic-N-Cu interactions [7]. To further investigate the stability of Cu_2O, SEM images of the three catalysts after CO_2RR were shown in Fig. S5. It is observed that Cu_2O on NRGO has the least morphology corruption compared with Cu_2O/RGO and pristine Cu_2O, indicating that NRGO indeed extends the durability of Cu_2O nanocubes. Further studies are needed to characterize the composition and morphology of Cu_2O catalysts in operando and to reveal the detailed synergetic mechanism of Cu_2O and pyridinic-N for boosting C_2H_4 selectivity by NRGO supports.

4. Conclusion

In summary, we developed a simple and potentially scalable synthetic protocol for preparation of Cu_2O nanocubes in situ supported on N-doped reduced graphene oxide as efficient catalyst for CO_2 electroreduction to ethylene. The Cu_2O loaded onto NRGO exhibits much higher C_2H_4 selectivity than Cu_2O loaded on RGO, as well as unsupported Cu_2O. The obtained Cu_2O/NRGO composite presents a high FE of C_2H_4 (19.7%) at −1.4 V (*vs.* RHE) with remarkable stability for at least 10000 s. The mass activity of Cu_2O on NRGO towards ethylene formation reaches as high as 136.1 mmol h^{-1} g^{-1}. We propose that the ultra-thin two-dimensional structure of NRGO facilitates the uniform dispersion of Cu_2O nanocubes, while the pyridinic-N moieties of NRGO can not only stabilize Cu_2O but also promote hydrogenation and carbon–carbon coupling reactions on Cu for the formation of C_2H_4. Further studies are needed to characterize the composition and morphology of Cu_2O catalysts in operando and to reveal the detailed synergetic mechanism between Cu_2O and pyridinic-N for boosting C_2H_4 selectivity. This work provides an effective and facile method to enhance the catalytic performance of Cu_2O for ethylene production by CO_2RR.

Acknowledgements

This work is financially supported by the National Natural Science Foundation of China (Nos. 21808242, 51572296, U1662113); the Financial Support from Taishan Scholar Project of Shandong Province of China.

Appendix A. Supplementary data

Supplementary data to this article can be found online at https://doi.org/10.1016/j.jallcom.2019.01.142.

References

[1] P.P. Yang, Z.J. Zhao, X.X. Chang, R.T. Mu, S.J. Zhan, G. Zhang, J.L. Gong, The functionality of surface hydroxy groups on the selectivity and activity of carbon dioxide reduction over cuprous oxide in aqueous solutions, Angew. Chem. Int. Ed. 57 (26) (2018) 7724–7728.

[2] C.T. Dinh, T. Burdyny, M.G. Kibria, A. Seifitokaldani, C.M. Gabardo, F. Pelayo García de Arquer, A. Kiani, J.P. Edwards, P. De Luna, O.S. Bushuyev, C.Q. Zou, R. Quintero-Bermudez, Y.J. Pang, D. Sinton, E.H. Sargent, CO_2 electroreduction to ethylene via hydroxide-mediated copper catalysis at an abrupt interface, Science 360 (2018) 783–787.

[3] S.Y. Lee, H. Jung, N.K. Kim, H.S. Oh, B.K. Min, Y.J. Hwang, Mixed copper states in anodized Cu electrocatalyst for stable and selective ethylene production from CO_2 reduction, J. Am. Chem. Soc. 140 (28) (2018) 8681–8689.

[4] C.C. Yan, H.B. Li, Y.F. Ye, H.H. Wu, F. Cai, R. Si, J.P. Xiao, S. Miao, S.H. Xie, F. Yang, Y.S. Li, G.X. Wang, X.H. Bao, Coordinatively unsaturated nickel–nitrogen sites towards selective and high-rate CO_2 electroreduction, Energy Environ. Sci. 11 (5) (2018) 1204–1210.

[5] B.H. Zhang, J.T. Zhang, Rational design of Cu-based electrocatalysts for electrochemical reduction of carbon dioxide, J. Energy Chem. 26 (6) (2017) 1050–1066.

[6] D. Raciti, C. Wang, Recent advances in CO_2 reduction electrocatalysis on copper, ACS Energy Lett. 3 (7) (2018) 1545–1556.

[7] H.J. Yang, H. Yang, Y.H. Hong, P.Y. Zhang, T. Wang, L.N. Chen, F.Y. Zhang, Q.H. Wu, N. Tian, Z.Y. Zhou, S.G. Sun, Promoting ethylene selectivity from CO_2 electroreduction on CuO supported onto CO_2 capture materials, Chemsuschem 11 (5) (2018) 881–887.

[8] Z.G. Zang, A. Nakamura, J.A. Temmyo, Single cuprous oxide films synthesized by radical oxidation at low temperature for PV application, Optic Express 21 (9) (2013) 11448–11456.

[9] Z.G. Zang, Efficiency enhancement of ZnO/Cu_2O solar cells with well oriented and micrometer grain sized Cu_2O films, Appl. Phys. Lett. 112 (4) (2018), 042106.

[10] C. Karthikeyan, K. Ramachandran, S. Sheet, D.J. Yoo, Y.S. Lee, Y.S. Kumar, A.R. Kim, G.G. Kumar, Pigeon-excreta-mediated synthesis of reduced graphene oxide (rGO)/$CuFe_2O_4$ nanocomposite and its catalytic activity toward sensitive and selective hydrogen peroxide detection, ACS Sustain. Chem. Eng. 5 (6) (2017) 4897–4905.

[11] J. Wei, Z.G. Zang, Y.B. Zhang, M. Wang, J.H. Du, X.S. Tang, Enhanced performance of light-controlled conductive switching in hybrid cuprous oxide/reduced graphene oxide (Cu_2O/rGO) nanocomposites, Opt. Lett. 42 (5) (2017) 911–914.

[12] K. Ramachandran, K.J. Babu, G.G. Kumar, A.R. Kim, D.J. Yoo, One-pot synthesis of graphene supported CuO nanorods for the electrochemical hydrazine sensor applications, Sci. Adv. Mater. 7 (2) (2015) 329–336.

[13] T.W. Zhou, Z.G. Zang, J. Wei, J.F. Zheng, J.Y. Hao, F.L. Ling, X.S. Tang, L. Fang, M. Zhou, Efficient charge carrier separation and excellent visible light photoresponse in Cu_2O nanowires, Nano Energy 50 (2018) 118–125.

[14] H. Mistry, A.S. Varela, C.S. Bonifacio, I. Zegkinoglou, I. Sinev, Y.W. Choi, K. Kisslinger, E.A. Stach, J.C. Yang, P. Strasser, B.R. Cuenya, Highly selective plasma-activated copper catalysts for carbon dioxide reduction to ethylene, Nat. Commun. 7 (2016) 12123.

[15] D. Ren, Y.L. Deng, A.D. Handoko, C.S. Chen, S. Malkhandi, B.S. Yeo, Selective electrochemical reduction of carbon dioxide to ethylene and ethanol on copper(I) oxide catalysts, ACS Catal. 5 (5) (2015) 2814–2821.

[16] M.I. Malik, Z.O. Malaibari, M. Atieh, B. Abussaud, Electrochemical reduction of CO_2 to methanol over MWCNTs impregnated with Cu_2O, Chem. Eng. Sci. 152 (2016) 468–477.

[17] H.Q. Li, N. Xiao, M.Y. Hao, X.H. Song, Y.W. Wang, Y.Q. Ji, C. Liu, C. Li, Z. Guo, F. Zhang, J.S. Qiu, Efficient CO_2 electroreduction over pyridinic-N active sites highly exposed on wrinkled porous carbon nanosheets, Chem. Eng. J. 351 (2018) 613–621.

[18] C.S. Cao, Z.H. Wen, Cu nanoparticles decorating rGO nanohybrids as electrocatalyst toward CO_2 reduction, J. CO_2 Util. 22 (2017) 231–237.

[19] Y.J. Huo, X.Y. Peng, X.J. Liu, H.Y. Li, J. Luo, High selectivity toward C_2H_4 production over Cu particles supported by butterfly-wing-derived carbon frameworks, ACS Appl. Mater. Interfaces 10 (15) (2018) 12618–12625.

[20] H. Ning, W.H. Wang, Q.H. Mao, S.R. Zheng, Z.X. Yang, Q.S. Zhao, M.B. Wu, Catalytic electroreduction of CO_2 to C_2H_4 using Cu_2O supported on 1-octyl-3-methylimidazole functionalized graphite sheets, Acta Phys. - Chim. Sin. 34 (8) (2018) 938–944.

[21] Q. Li, W.L. Zhu, J.J. Fu, H.Y. Zhang, G. Wu, S.H. Sun, Controlled assembly of Cu nanoparticles on pyridinic-N rich graphene for electrochemical reduction of CO_2 to ethylene, Nano Energy 24 (2016) 1–9.

[22] W. Yin, H.X. Lin, Y.F. Zhang, X. Huang, W.K. Chen, Density functional theory study of IB metals binding to perfect and N-doped graphene, Chin. J. Catal. 33 (9) (2013) 1578–1585.

[23] P. Sekar, L. Calvillo, C. Tubaro, M. Baron, A. Pokle, F. Carraro, A. Martucci, S. Agnoli, Cobalt spinel nanocubes on N-doped graphene: a synergistic hybrid electrocatalyst for the highly selective reduction of carbon dioxide to formic Acid, ACS Catal. 7 (2017) 7695–7703.

[24] Song, Y., Peng, R., Hensley, D.K., Bonnesen, P.V., Liang, L.B., Wu, Z.L., Meyer, H.M., Chi, M.F., Ma, C., Sumpter, B.G., Rondinone, A.J., High-selectivity electrochemical conversion of CO_2 to ethanol using a copper nanoparticle/N-doped graphene electrode. ChemistrySelect. 1, 1-8.

[25] T.T. Zhuang, Z.Q. Liang, A. Seifitokaldani, Y. Li, P. De Luna, T. Burdyny, F.L. Che, F. Meng, Y.M. Min, R. Quintero-Bermudez, C.T. Dinh, Y.J. Pang, M. Zhong, B. Zhang, J. Li, P.N. Chen, X.L. Zheng, H.Y. Liang, W.N. Ge, B.J. Ye, D. Sinton, S.H. Yu, E.H. Sargent, Steering post-C–C coupling selectivity enables high efficiency electroreduction of carbon dioxide to multi-carbon alcohols, Nat. Catal. 1 (6) (2018) 421–428.

[26] D. Liu, C.P. Fu, N.S. Zhang, Y.L. Li, H.H. Zhou, Y.F. Kuang, Porous nitrogen-doped graphene for high energy density supercapacitors in an ionic liquid electrolyte, J. Solid State Electrochem. 21 (3) (2017) 759–766.

[27] M. Vinothkannan, C. Karthikeyan, G.G. Kumar, A.R. Kim, D.J. Yoo, One-pot green synthesis of reduced graphene oxide (RGO)/Fe_3O_4 nanocomposites and its catalytic activity toward methylene blue dye degradation, Spectrochim. Acta 136 (2015) 256–264.

[28] M. Vinothkannan, A.R. Kim, G.G. Kumar, D.J. Yoo, Sulfonated graphene oxide/Nafion composite membranes for high temperature and low humidity proton exchange membrane fuel cells, RSC Adv. 8 (14) (2018) 7494–7508.

[29] Z.Y. Lin, Y.G. Yao, Z. Li, Y. Liu, Z. Li, C.P. Wong, Solvent-assisted thermal reduction of graphite oxide, J. Phys. Chem. C 114 (35) (2010) 14819–14825.

[30] Y. Zhang, X. Wang, L. Zeng, S.Y. Song, D.P. Liu, Green and controlled synthesis of Cu_2O-graphene hierarchical nanohybrids as high-performance anode materials for lithium-ion batteries via an ultrasound assisted approach, Dalton Trans. 41 (15) (2012) 4316–4319.

[31] D.H. Lim, J.H. Jo, D.Y. Shin, J. Wilcox, H.C. Ham, S.W. Nam, Carbon dioxide conversion into hydrocarbon fuels on defective graphene-supported Cu nanoparticles from first principles, Nanoscale 6 (10) (2014) 5087–5092.